



OPEN ACCESS

EDITED BY

Nick Varley,
University of Colima, Mexico

REVIEWED BY

Maurizio Mulas,
ESPOL Polytechnic University, Ecuador
Kazutaka Mannen,
Hot Springs Research Institute of Kanagawa
Prefecture, Japan

*CORRESPONDENCE

Susanna F. Jenkins,
✉ susanna.jenkins@ntu.edu.sg

RECEIVED 26 February 2024

ACCEPTED 19 July 2024

PUBLISHED 15 August 2024

CITATION

Jenkins SF, McSporran A, Wilson TM,
Stewart C, Leonard G, Cevuard S and
Garaebiti E (2024) Tephra fall impacts to
buildings: the 2017–2018 Manaro Voui
eruption, Vanuatu.

Front. Earth Sci. 12:1392098.

doi: 10.3389/feart.2024.1392098

COPYRIGHT

© 2024 Jenkins, McSporran, Wilson, Stewart,
Leonard, Cevuard and Garaebiti. This is an
open-access article distributed under the
terms of the [Creative Commons Attribution
License \(CC BY\)](https://creativecommons.org/licenses/by/4.0/). The use, distribution or
reproduction in other forums is permitted,
provided the original author(s) and the
copyright owner(s) are credited and that the
original publication in this journal is cited, in
accordance with accepted academic practice.
No use, distribution or reproduction is
permitted which does not comply with
these terms.

Tephra fall impacts to buildings: the 2017–2018 Manaro Voui eruption, Vanuatu

Susanna F. Jenkins^{1*}, Ame McSporran², Thomas M. Wilson²,
Carol Stewart³, Graham Leonard⁴, Sandrine Cevuard⁵ and
Esline Garaebiti⁵

¹Earth Observatory of Singapore, Asian School of the Environment, Nanyang Technological University, Singapore, Singapore, ²School of Earth and Environment, University of Canterbury, Christchurch, New Zealand, ³School of Health Sciences, Massey University, Wellington, New Zealand, ⁴GNS Science, Lower Hutt, New Zealand, ⁵Vanuatu Meteorology and Geohazards Department, Port Vila, Vanuatu

Building damage from tephra falls can have a substantial impact on exposed communities around erupting volcanoes. There are limited empirical studies of tephra fall impacts on buildings, with none on tephra falls impacting traditional thatched timber buildings, despite their prevalence across South Pacific island nations and parts of Asia. The 2017/2018 explosive eruption of Manaro Voui, Ambae Island, Vanuatu, resulted in damage to traditional (thatched timber), non-traditional (masonry), and hybrid buildings from tephra falls in March/April and July 2018. Field and photographic surveys were conducted across three separate field studies with building characteristics and damage recorded for a total of 589 buildings. Buildings were classified using a damage state framework customised for this study. Overall, increasing tephra thicknesses were related to increasing severity of building damage, corroborating previous damage surveys and vulnerability estimates. Traditional buildings were found to be less resistant to tephra loading than non-traditional buildings, although there was variation in resistance within each building type. For example, some traditional buildings collapsed under ~40 mm thickness while others sustained no damage when exposed to >200 mm. We attribute this to differences in the pre-eruption condition of the building and the implementation of mitigation strategies. Mitigation strategies included covering thatched roofs with tarpaulins, which helped shed tephra and consequently reduced loading, and providing an internal prop to the main roof beam, which aided structural resistance. As is typical of post-event building damage surveys, we had limited time and access to the exposed communities, and we note the limitations this had for our findings. Our results contribute to the limited empirical data available for tephra fall building damage and can be used to calibrate existing fragility functions, improving our evidence base for forecasting future impacts for similar construction types globally.

KEYWORDS

tephra fall, eruption impacts, building damage, impact assessment, ambae eruption

1 Introduction

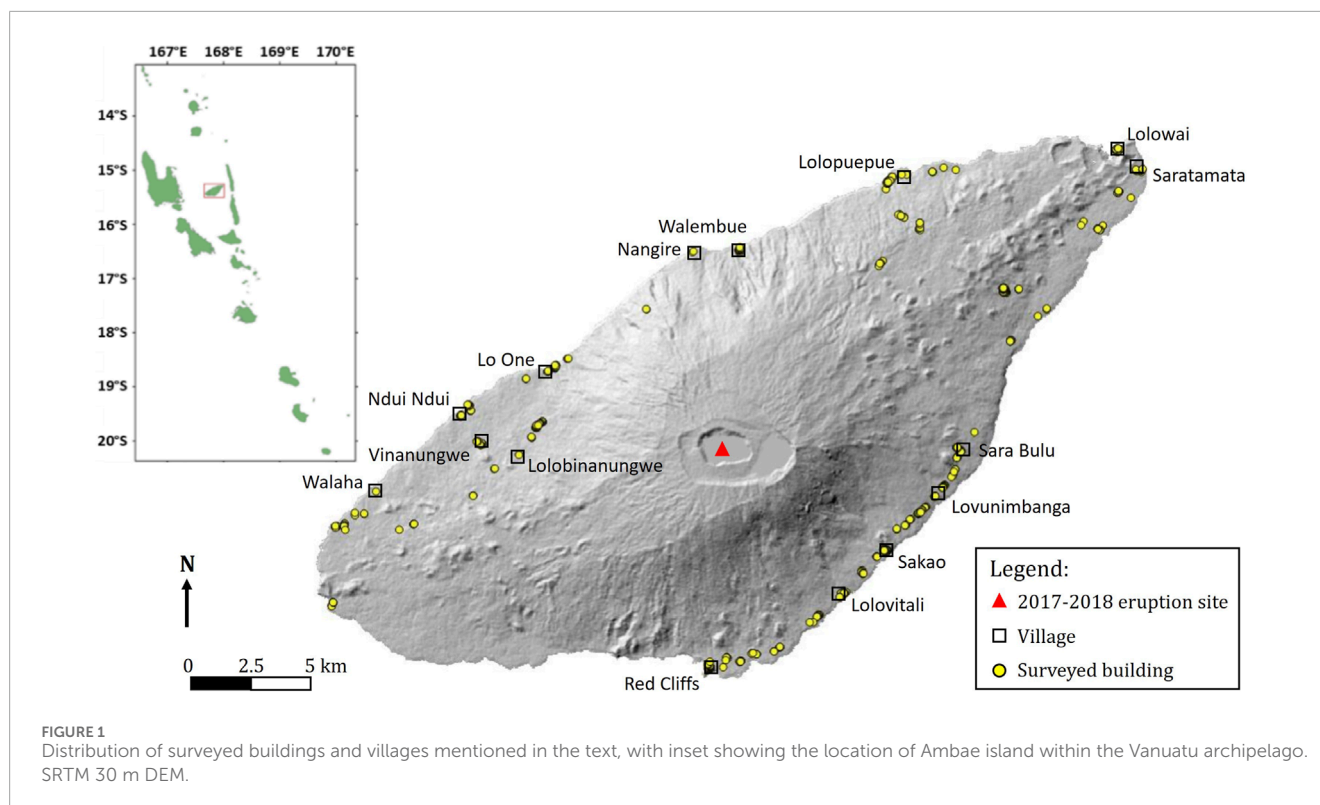
Tephra fall is one of the most widespread and common volcanic hazards, with wide-ranging impacts that include building damage and destruction (Blong, 1981; Jenkins et al., 2014). The impact of tephra falls on buildings can reduce their ability to provide safe and functional habitation for occupants, influencing many aspects of community response to eruptions; for example, the decision to temporarily evacuate or permanently relocate during an eruption crisis (Deligne et al., 2017; Lechner and Rouleau, 2019; Martinez-Villegas et al., 2021). Typical impacts of tephra falls on buildings include: i) structural damage caused by static loading, ii) damage to non-structural elements (e.g., gutters, painting, roof cladding) caused by loading or corrosion, iii) damage or disruption of building services (e.g., air-conditioning systems, water supplies), and iv) contamination of building interiors and exteriors that requires clean-up and affects safe occupation (e.g., Blong, 1984; Spence et al., 1996; Pomonis et al., 1999; Blong, 2003; Spence et al., 2005; Hayes et al., 2019). While the importance of tephra fall impacts for buildings is well recognised, our understanding of the impacts draws from a very limited evidence base. To date, for building damage from tephra fall there are only two dedicated field studies, plus one interpretation of government-gathered field data and one remote satellite-image study in the literature, compared to more than 600 building damage surveys for earthquakes (Spence et al., 2011). In part this is because of the relatively rarity of tephra falls that damage populated areas, but also the challenging nature of volcanic crises, which can extend for many days, months or even years (Siebert et al., 2015), making timely access to impacted areas very difficult, if not impossible.

Field surveys of tephra fall building damage have been carried out in Castillejos following the 1991 eruption of Pinatubo, Philippines ($n = 51$ buildings; Spence et al., 1996) and in Rabaul following the 1994 eruptions of Tavurvur and Vulcan, Papua New Guinea ($n = 173$ buildings; Blong, 2003). Hayes et al. (2019) used damage data collected by a government agency to assess damage for communities around Calbuco, Chile, following the 2015 eruption ($n = 417$ buildings). A fourth field survey has been carried out following the 2021 Soufrière St Vincent eruption (Miller et al., 2023) with damage categorisation and analyses ongoing at the time of writing. Williams et al. (2020) conducted a remote damage assessment of the Kelud 2014 tephra falls using satellite imagery to categorise damage for 1,154 buildings, providing a complementary way of supplementing our limited empirical damage dataset. Empirical data sourced from these surveys have been used alongside expert judgement and theoretical calculations to develop quantitative vulnerability and fragility functions that inform how buildings of various construction types will respond to future tephra falls (e.g., Spence et al., 2005; Jenkins et al., 2014; Williams et al., 2020). Such functions relate the hazard intensity (e.g., tephra fall load) to the response of a building (e.g., level of damage); however, given the limited empirical data, they are typically the most uncertain and least developed element of a volcanic risk assessment (Deligne et al., 2022), especially when compared to vulnerability estimates used in earthquake or flood risk models.

While these seminal tephra fall building damage surveys have been invaluable in improving the quality of building damage

estimates in the event of a future eruption, such estimates typically focus on a small number of building typologies, which are dominated by engineer-designed and -approved buildings typical of more developed countries (e.g., Pomonis et al., 1999; Marti et al., 2008; Zuccaro et al., 2008). The explosive eruption of Manaro Voui Volcano, Ambae, Vanuatu, in 2017–2018 provided an opportunity to expand the empirical database of tephra fall impacts addressing some key knowledge gaps. Firstly, there has been very limited focus on the impact of tephra on traditional non-engineered thatched buildings constructed from forest materials such as bamboo, un-milled timber (e.g., tree trunks or branches) and foliage, despite their strong prevalence in some communities in tropical environments, such as Ambae and other islands of the South Pacific. The one exception is that of Jenkins et al. (2015), who used expert judgement and structural engineering calculations to derive vulnerability functions that estimated failure of traditional Nipa (palm) thatched dwellings in the Philippines under tephra fall loads of 1–2.1 kPa (10th to 90th percentile, with a mean load of 1.4 kPa). To the best of our knowledge, empirical post-eruption damage data for traditional thatched buildings (hereafter referred to as traditional buildings) have not been collected and thus tephra fall vulnerability estimates for such buildings are less robust than for non-traditional and engineered building types. Understanding traditional building vulnerability from tephra fall is particularly important for island nations to aid emergency shelter planning as their isolation and small landmasses can make rapid evacuation or relocation difficult (Shultz et al., 2016), potentially putting the lives of those who shelter in place in danger. Secondly, we were able to collect empirical data on the damage to buildings that are not traditional, such as those with metal sheet roofs, adding to the existing dataset. Finally, we focussed on cataloguing the direct impacts i.e., damage and destruction, of tephra fall on buildings and building support systems such as gutters but also assessed the indirect impacts of tephra on building functionality and habitability as well as the mitigation strategies employed to reduce impacts of tephra fall on buildings. Indirect impacts from tephra remobilisation have previously been recognised (e.g., Wilson et al., 2011; Craig et al., 2016; Dominguez et al., 2020), and we provide further empirical data here. Tephra impacts on societal habitability were the primary motivation for the government-mandated whole-island evacuation of Ambae following the July 2018 tephra falls (Rovins et al., 2020) and the impacts to water and air quality are presented in a partner paper (Stewart et al., in prep.).

We provide background to Ambae's population and built environment in Section 2, as well as Manaro Voui's eruption history, the 2017/2018 eruption and its tephra falls. The Methodology section describes our photographic building survey and the collection of associated field observation data during three field visits to Ambae in 2018, which were used to compile a geospatial building inventory of typology and damage for the two main tephra fall phases (March/April and July). The Results section presents an overview of the building typologies surveyed on Ambae and the relationship observed between building damage and tephra fall thickness. We then discuss these results, damage mechanisms and modes, as well as observations of tephra contamination of interiors and mitigation measures that were employed to limit impact.



2 Island and eruption overview

The island of Ambae represents the emergent summit of Manaro Voui, a geologically active basaltic shield volcano, with rocks dating back to at least 1.7 million years (Warden, 1970). It is Vanuatu's largest volcano and rises 3,900 m from the seabed to an elevation of 1,496 m above sea level (Cronin et al., 2004). Manaro Voui is elongated along a SW to NE-trending magmatic rift zone. Scoria cones scatter the rift zone, marking the sites of previous fissure-style eruptions (Robin et al., 1993). A large-scale eruption approximately 400 years ago built the present summit calderas occupied by Lake Voui, Manaro Lakua and Manaro Ngoro (Warden, 1970; Rouland et al., 2001) with the current active vent located below central Lake Voui (Figure 1). Since then, Manaro Voui's activity has been characterised by multiple explosive eruptions, lahars and gas-release events (Cronin et al., 2004) with notable eruptions around 1575, 1670, 1870, 1995, 2005–2006, 2011, 2016 and 2017/2018.

Prior to the 2017/2018 eruptive period of Manaro Voui, Ambae's population was approximately 11,000 (VNSO, 2016), most of whom live along the coastline in small villages (Figure 1). Ambae residents are largely self-sufficient with respect to their food supplies. The main source of income for 59% of Ambae households is the sale of cash and food crops, fish and handcrafts (VNSO, 2016).

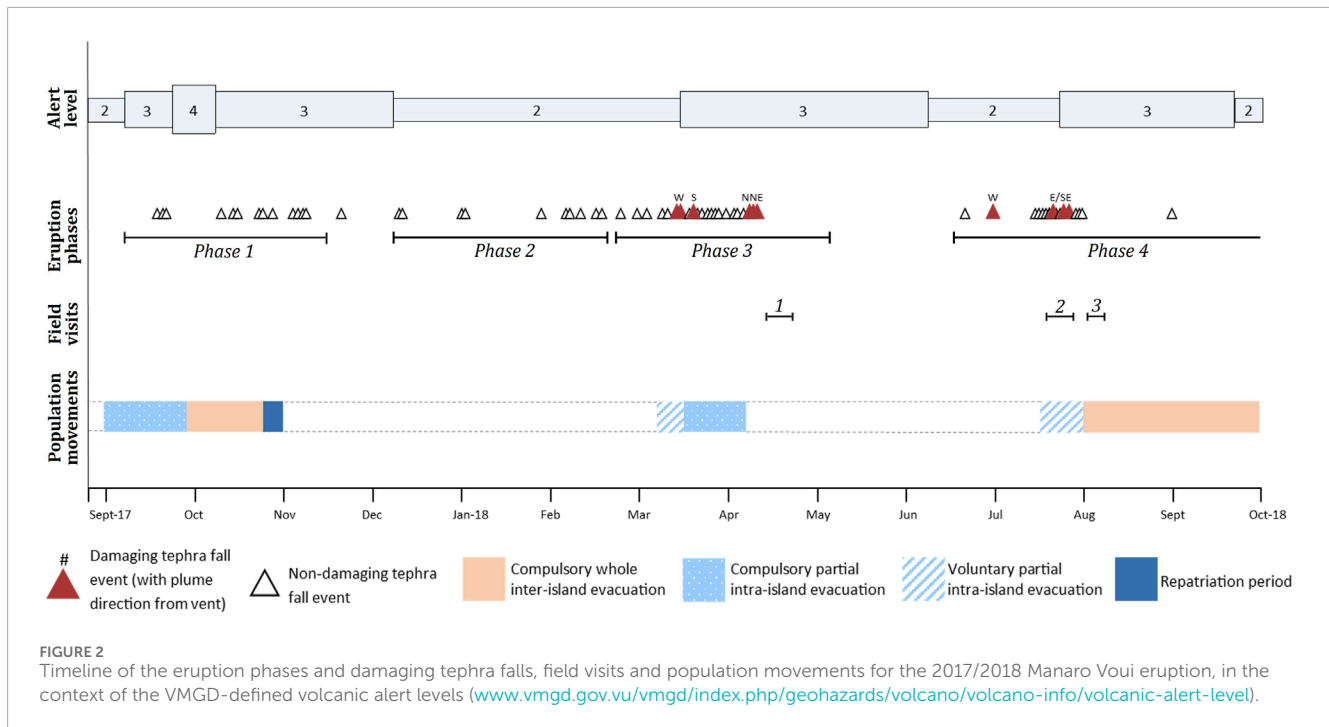
2.1 Manaro Voui 2017/2018 eruption

The eruptive period that began in September 2017 is part of a much longer sequence that began with volcanic unrest

in 1991 followed by eruptions in 1995, 2005–2006, and 2011. The 2017/2018 eruptive period, designated Volcanic Explosivity Index (VEI) 3, has been split into four phases by the Vanuatu Meteorology and Geohazards Department (Vanuatu Meteorology and Geohazards Department, 2018), shown in Figure 2 alongside tephra falls, population movements and the Vanuatu Meteorology and Geohazards Department (VMGD)-defined volcanic alert levels, which range from 0 (no signs of change in activity) to 5 (danger beyond caldera, on entire and surrounding islands, and also chance of flank eruption). There were more than 60 individual tephra falls during the 2017/2018 eruptive period; however, only ten reached populated areas and caused damage to buildings: six in March and April 2018, and four in July 2018 (Figure 2). We carried out field impact assessments, at the request of the Vanuatu Meteorology and Geohazards Department, in April, July and August 2018 (Figure 2).

Phase 1, from September to November 2017, involved a series of moderate phreatic eruptions with low-level plume heights (mostly to a few kilometres a.s.l. and exceptionally to 9.1 km a.s.l.) that caused the evacuation of more than 8,000 people (Global Volcanism Program, 2018a), and resulted in tephra falls on, but no reported damage to, buildings on Ambae. This phase prompted a total evacuation of the island between 29 September and 21 October 2017 (Rovins et al., 2020), which was largely due to fears of eruption escalation based on previous eruptive activity at Manaro Voui.

Phase 2 between December 2017 and February 2018 represented a period of less frequent explosions with plume heights up to 4.6 km a.s.l. Heightened degassing produced acid rain to the west of the active vent. A tephra plume to 3.1 km a.s.l. on 8 January



resulted in reports of tephra falls in the north and north-east of the island (Global Volcanism Program, 2018b).

Phase 3, between March and May 2018, produced acid rain to the west and multiple tephra falls, which increased in volume and frequency through March, with plume heights to 6.1 km a.s.l. Six distinct tephra falls during Phase 3 resulted in damage to buildings and prompted an intra-island evacuation from the exposed areas, primarily to the eastern end of the island. During this phase, the Category 2 Tropical Cyclone Hola hit Ambae (7–8 March 2018) causing heavy rainfalls that continued through March causing a lahar that damaged Waluembue village in the north of Ambae (Global Volcanism Program, 2018b).

Phase 4, from June–November 2018, produced plume heights to 12 km a.s.l. and brought further thick tephra falls to the west, east and southeast, causing major damage to crops, water supplies and traditional buildings. This prompted another government-mandated whole-island evacuation from the end of July until the end of October 2018, when volcanic activity ceased and the State of Emergency lifted on 26 November 2018 (Rovins et al., 2020).

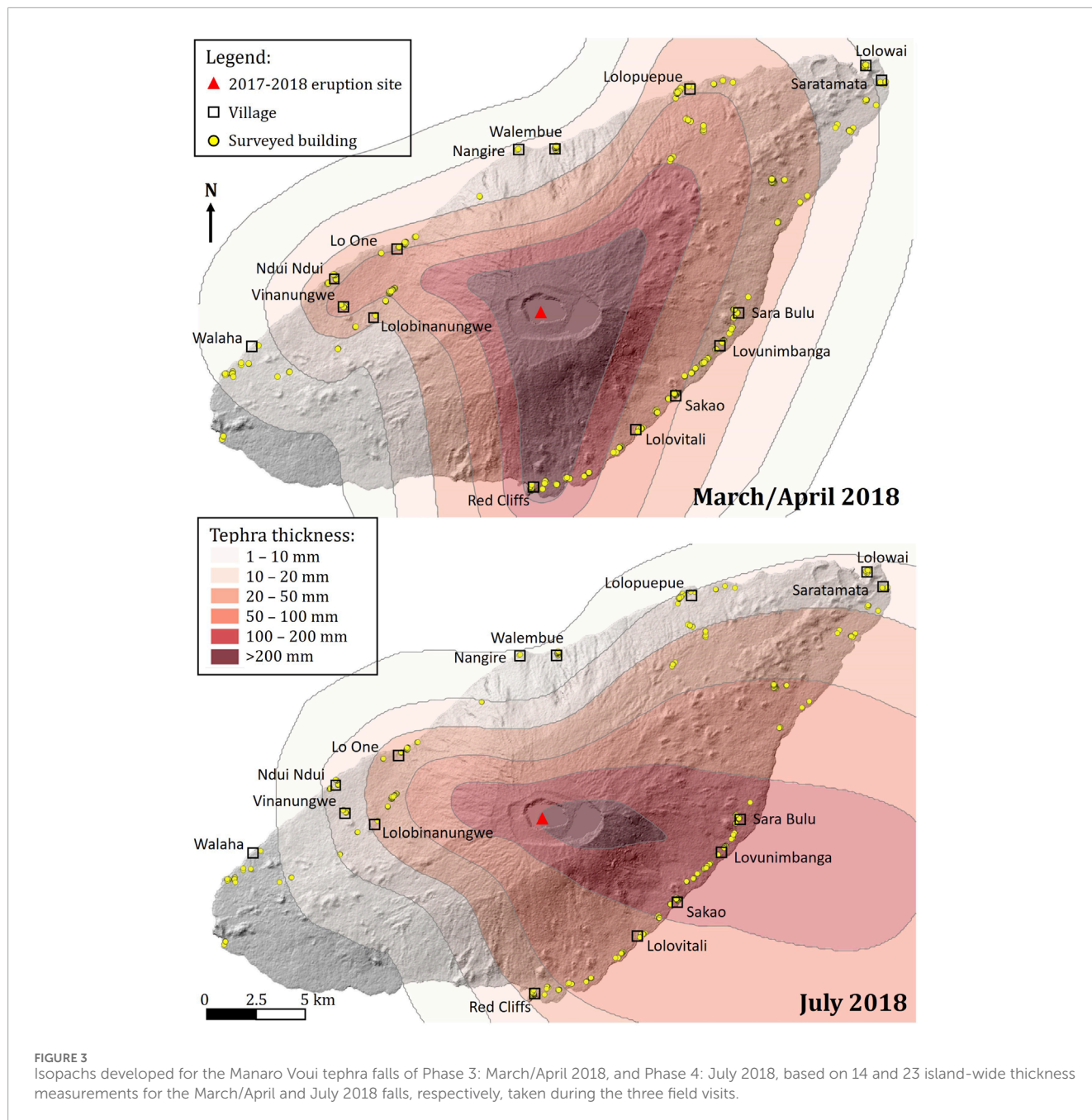
Isopachs representing the aggregated distribution and thickness of damaging tephra falls from Phases 3 (March/April; $n = 6$) and 4 (July 2018; $n = 4$) show that while the very southwestern tip of the island received little to no tephra fall, most of the island was affected at some point during the March/April and July 2018 tephra falls (Figure 3). Of the affected villages, thicker fall deposits were experienced to the south (Red Cliffs: >200 mm) during the March/April phase, and to the east (Lovunimbanga: ~170 mm) in the July phase (Figure 3). Phase 3 and 4 tephras were clearly and consistently distinguishable across the deposits, with the lower March/April deposits characterised in the field and analysed post-trip by University of Canterbury and GNS Science

as light brown sand-sized tephra (250–1,000 μm) and the upper July deposits as dark grey silt to fine-grained sand-sized tephra (<125 μm).

When considering building damage, a more appropriate tephra fall hazard intensity metric than thickness or grain size is the load - a function of the deposit thickness and density (Spence et al., 1996; Blong, 2003; Jenkins et al., 2014). Two deposit bulk density measurements were taken *in situ* by other members of the field team, both in Lolovitali, approximately 7 km southeast of the vent, during the same prolonged tephra fall of 21–22 July 2018. A further 15 deposits were collected in the field during the second field visit in July with density measurements made later in the laboratory. Deposit densities of 970 kg/m^3 and 440 kg/m^3 were measured *in situ* after 7.5 and 15.5 h of tephra fall, respectively. Densities measured in the laboratory from samples range from 900 kg/m^3 to 1,680 kg/m^3 , with no clear orientation towards higher or lower densities associated with either the phase, collection location or calculation method. Given this wide range, we chose only to interpret building damage as a function of thickness for this study to avoid additional uncertainty in hazard intensity.

3 Methodology

During three field visits to Ambae, we focussed on collecting building typology and impact data for the March/April and July 2018 tephra falls that caused damage to buildings. While data were also collected on impacts to crops, infrastructure, drinking water and air quality, including during an additional field trip in March 2018 (Stewart et al., in prep.), here we present our data for buildings only. Field visit 1 (17–21 April 2018) followed a government-mandated



intra-island evacuation, Field visit 2 (18–25 July 2018) took place during a voluntary intra-island evacuation and field visit 3 (4–9 August 2018) took place just prior to a government-ordered whole-island evacuation. Thus, for all three trips there were people living in affected areas. The field teams were all experienced with gathering data in a syn-/post-disaster setting, and thus exercised sensitivity; trips always included a VMGD staff member who (amongst many things) guided respect of local customs and translation.

The first and third field visits were led by the Vanuatu Meteorology and Geohazards Department (VMGD), who requested international collaboration to assist with the humanitarian response. The New Zealand Ministry of Foreign Affairs and Trade part-

funded an international field team to join VMGD scientists on Ambae to address concerns about roof collapse, crop damage and impacts on drinking water and air quality (Table 1). The second field visit was part of a longitudinal study of the 2017/2018 Manaro Voui eruptive period by a team interested in the physical eruption processes and tephra fall characteristics (Table 1). Given the limited time available during visits 1 and 2, we employed photographic surveys of buildings. During visit 3, we carried out a systematic building-by-building field survey in impacted areas. A photographic survey involves taking multiple georeferenced photographs of a building exterior and interior, to be later geolocated and categorised using satellite imagery and field notes. These were either employed

TABLE 1 Summary of the focus, data collection for buildings, and timing of the three field visits to Ambae in 2018 relative to the eruption phases and damaging tephra falls.

| Field visit and focus | Data collected | Dates on Ambae (2018) | Days since damaging tephra falls |
|--|---|-----------------------|---|
| Phase 3: February to April 2018, comprising six damaging tephra falls | | | |
| Field visit 1—International humanitarian support | • Building photographic surveys (n = 23) | 17–21 April | <ul style="list-style-type: none"> • 34 days since 15–16 March damaging tephra falls (n = 2) to the West • 30 days since 21 March damaging tephra fall (n = 1) to the South • 9 days since 9–11 April damaging tephra falls (n = 3) to the North-Northeast |
| Phase 4: July to November 2018, comprising four damaging tephra falls | | | |
| Field visit 2—Longitudinal physical volcanology research | • Building photographic surveys (n = 131) | 18–25 July | <ul style="list-style-type: none"> • 22 days since 1 July damaging tephra fall (n = 1) to the West • Present during 16–25 July damaging tephra falls (n = 3) to the East-Southeast |
| Field visit 3—International humanitarian support | • Building systematic surveys (n = 435) | 4–9 August | <ul style="list-style-type: none"> • 35 days since 1 July damaging tephra fall (n = 1) to the West • 14 days since 16–25 July damaging tephra falls (n = 3) to the East-Southeast |

in isolation (visits 1 and 2) or were supplementary to systematic building surveys in the field (visit 3). Photographic surveys were beneficial as they allowed for greater spatial coverage across Ambae given the limited time available for damage surveying. Photographic surveys typically took a few minutes per building, longer if there was unusual or extensive damage, while systematic building surveys took up to an hour or more per building, depending on the nature and extent of damage. For surveying, we focussed on accessible areas with known tephra fall impacts, and made efforts to map from trace to heavy ash fall to capture the range. In total, across these three visits, 589 buildings were assessed for damage with the building construction type, condition, and approximate age of each building noted where possible. We also qualitatively assessed how, and how much, tephra had ingressed into a building, where appropriate, along with any efforts to mitigate damage or contamination.

3.1 Building typologies

Broad categories and more detailed subcategories of building material and construction style on Ambae were defined following the first field visit in mid-April 2018 and refined during the third field visit in early August 2018. While we collected building data during each of the three surveys, the vast majority were obtained during the third survey in August 2018 (n = 435) as this included a dedicated and systematic building damage assessment (Table 1). Defined categories record the principal typology of the wall and roof frame (e.g., timber, reinforced concrete), the wall and roof material (e.g., thatched, metal) as well as further characteristics, such as roof pitch, usage and the presence of verandas, gutters and so forth. In total, a geospatial inventory of 589 buildings impacted by tephra fall was developed (Supplementary Material S1), with each building assigned information for the typology and characteristics described above as well as the location (from GPS and/or satellite imagery), ID, survey number, and the number and orientation of geolocated photographs.

3.2 Building damage

Tephra fall damage, or lack of damage, visible from field observations and photographs was recorded and a damage state allocated for each building (Table 2; Figure 4). Each building was assigned a binned tephra fall thickness based upon the isopachs developed for the March/April and July 2018 tephra fall phases (Figure 3). Photographs from the first field visit, undertaken between 9 and 34 days after the damaging tephra falls of the March/April phase, showed that many building roofs across the island had already been, or were in the process of, being cleared of tephra. We have therefore assumed that any tephra that accumulated on a roof during the March/April 2018 tephra falls was removed (by people, wind and/or rain) before the July 2018 tephra falls. Thus, building damage was associated with a tephra fall thickness from *either* the March/April or the July falls, rather than an accumulation of the two or only the July 2018 falls. This has the effect of being conservative, in that the individual phase, rather than cumulated multi-phase, tephra thickness is recorded.

We used a damage state scheme similar to that of Hayes et al. (2019), which itself was a slightly adapted version of the schemes used by Blong (2003); Spence et al. (1996). Our adaptations made damage observations more relevant to Ambae building typologies, by omitting features such as electrical systems, air conditioning units and tiled roofs. The damage states are ordinal, in that the characteristics of a certain damage state include those of lower, less severe damage states. We retained the philosophy behind previous approaches to damage states, where the highest damage state (DS5) is related to roof collapse. Roof, rather than building, collapse is not necessarily analogous to complete destruction from an economic perspective (i.e., full building collapse), but it does relate to the maximum threat to life safety and habitability, which was our focus in this case. Where a building exhibited multiple damage characteristics across different damage states, the highest damage state was assigned. In addition to cataloguing the damage to each surveyed building, we noted observations of tephra infiltration into,

TABLE 2 Building damage state framework used to categorise building damage from the 2017/18 Manaro Voui eruption, adapted from Hayes et al. (2019). A damage state is achieved if any of the characteristics are present; where multiple damage characteristics exist that are across different damage states, the higher damage state is assigned.

| Damage state | Description | Characteristics |
|--------------|---|---|
| DS0 | No Damage | <ul style="list-style-type: none"> No Damage |
| DS1 | Light damage or damage to non-structural elements | <ul style="list-style-type: none"> Damage to gutters Damage to contents Dents or minor slumping in roof cover |
| DS2 | Moderate damage but vertical structure and roof supports intact | <ul style="list-style-type: none"> As for DS1, plus Bending or excessive damage (without collapse) to up to half of the roof covering Little or no damage to roof support trusses and rafters Damage to roof overhangs or verandas Interior requires repair |
| DS3 | Severe damage to the roof and supports | <ul style="list-style-type: none"> As for DS2, plus Bending or excessive damage (with or without collapse) to more than half of the roof covering Damage to any single principal roof supports and/or some damage to walls (less than half of walls affected) Severe damage or partial collapse of roof overhangs or verandas |
| DS4 | Partial collapse of the roof and supports | <ul style="list-style-type: none"> As for DS3, plus Collapse to less than half of roof covering and principal roof support(s) At least half of external and/or internal walls deformed or collapsed |
| DS5 | Building collapse | <ul style="list-style-type: none"> As for DS4, plus Collapse of roof, principal roof supports and/or supporting external walls over more than half of floor area of building |



and contamination of, building interiors. We also noted observations of mitigation strategies being used by residents to reduce the impacts of the tephra falls on buildings. These included fastening of tarpaulins over roofs and openings, roof beams being braced by an emergency prop, and the pre-emptive removal of roof guttering (used for collecting rainwater, as the sole source of drinking water supply) prior to tephra falls.

4 Results

4.1 Building typologies

Four broad building construction typologies, and nine subcategories, were identified from field studies and photographs for the 589 surveyed buildings on Ambae (Figure 5; Table 3). In addition to informing our damage assessment, these typologies can be used in developing exposure models for forecasting future impacts. Traditional short-span (Ts) buildings, with locally-sourced timber or bamboo frame, split bamboo wall cladding and a thatched roof, were the most prevalent of the surveyed building types ($n = 255$; 43%), followed by unreinforced breeze block masonry walls with a timber framed roof and corrugated sheet metal roof cover (Nb) ($n = 161$; 27%). Together they comprised 71% ($n = 416$ out of 589) of the surveyed building stock, with mixed construction (Xw, $n = 76$; 13%) and timber frame (Nt, $n = 47$; 8%) representing a further 21%. The remaining 50 buildings (8%) comprised metal sheet-timber hybrid buildings ($n = 27$; 5%), evacuation shelters ($n = 13$; 2%), reinforced concrete frame buildings ($n = 6$; 1%), and traditional outhouses ($n = 4$; <1%). Temporary canvas shelters were erected as evacuation shelters following phases 1 through 3, and assessed in Lo One and near Walaha only during the third field visit in August. All buildings were constructed for the tropical climate, with ventilation pathways observed between external walls and roof.

The spatial distribution of building construction typologies varied across our survey locations. A greater proportion of non-traditional, typically more modern, buildings were observed in villages with schools, health centres, churches and general stores, such as Lolowai and Lolopuepue in the more populated northeastern tip of the island, which contains the airport, main port and the capital of Penama province (Saratamata). There were no traditional buildings observed during a full village survey of Lolowai. By contrast, traditional construction buildings dominated in more rural villages to the west and south/southeast of the island. For example, they made up more than 50% of the building stock in Lovunimbanga and Sakao in the southeast and Lolombinangwe and Vinanungwe in the west (Figure 1). As tephra thicknesses were greater in the South (March–April) and East (July) of the island and thinner in the North (Figure 3), traditional buildings dominate the greater tephra thicknesses (>100 mm) and non-traditional the thinner tephra thicknesses (<50 mm) (Figure 6). We observed tephra ‘crusts’ in Sara Bulu village in the east of the island, where we know there was at least one rainfall event between tephra fall deposition and thickness measurement. In the west of the island, which experienced no intervening rains, no crust was observed.

4.2 Building damage

Of the 589 buildings surveyed on Ambae, just over half ($n = 332$, 56%) showed no signs of damage (DS0) with a further 23% ($n = 134$) sustaining minor damage (DS1). Partial or complete roof collapse (DS4–5) was observed for 12% ($n = 71$) of surveyed buildings, 83% ($n = 59$) of which were traditional construction (Table 4), despite traditional buildings comprising less than half (44%; $n = 259$) of the dataset (Table 3). Hybrid buildings with traditional roofs (X1) appeared to suffer less damage than hybrid buildings with traditional walls (X2), although the number of data were few (7 and 20 buildings, respectively). Mixed wall hybrid buildings (Xw) appeared to show similar levels of damage to non-traditional timber frame buildings (Nt), which is expected given that the only key difference between the two typologies is a basal half wall of breeze blocks (Xw) (Table 3, 4).

Buildings sustained greater damage in areas that received more tephra fall (Figures 7A, C), with tephra falls ≥ 100 mm associated with 70% (50 out of 71) of the buildings assigned partial or total collapse, DS4/5. Higher damage states were observed for traditional short span buildings (Ts), compared to non-traditional buildings (Nt, Nb, Nc) (Figure 7B) although tephra thicknesses were larger at surveyed traditional buildings (Figure 7D).

Figure 8 helps to differentiate the influence of tephra thickness on damage from that of building typology on damage, with the proportion of damage states within each tephra thickness bin shown separately for the broad building typologies. We found that different building typologies experienced different levels of damage under the same tephra thicknesses, i.e., that building typology affects a building’s vulnerability to tephra fall loading. However, because of the spatial distribution of building types relative to tephra falls, data are not equally spread between tephra thickness bins and some categories have very few data (e.g., reinforced concrete frame buildings, Nc, $n = 6$: Figures 7B, D).

4.3 Non-structural impacts

Gutter damage was the most common form of damage to non-structural elements (DS1) observed on Ambae. Gutters were metal or plastic and attached to the roof using U hooks. They were only found on buildings with corrugated sheet metal roofs, i.e., hybrid or non-traditional buildings, though not all such roofs had gutters. Of the 134 DS1 buildings, 31 (23%) exhibited gutter damage or failure. Typically, the U hook fastening between gutter and building was damaged or failed, rather than the gutter itself. The minimum and maximum tephra thickness at which gutter damage was observed was 1 mm and 228 mm, respectively, with a median of 83 mm and mean of 92 mm. The load that a tephra deposit places on a gutter is affected by the tephra thickness, source roof area as well as the moisture content and density of the deposit.

While typically not causing damage, wind remobilisation of tephra deposits into buildings was observed for all buildings and required clean-up. As an example, we observed tephra infiltration inside two unreinforced masonry block (Nb) schools with metal sheet roofs and louvre windows in Lovunimbanga and Nangire villages, ~ 10.5 km due east and ~ 8 km due north of the 2017–2018 active vent respectively. Lovunimbanga received tephra falls of



FIGURE 5
Four principal building construction typologies present on Ambae at the time of the 2017/2018 eruption: Traditional (T), Hybrid construction (X), Non-traditional construction (N) and Temporary (E).

around 40 mm, and ~ 0.5 mm was found inside the surveyed school, while Nangire received tephra falls around one order of magnitude smaller at ~ 4 mm, but a similar thickness of ~ 0.5 mm was found inside the surveyed school. The only marked difference between the buildings was that the louvre windows were closed in Lovunimbanga but open in Nangire; however, the north and west of the island are typically drier than the south and east because of tradewinds so the tephra fall surface and moisture content could also be a factor. The thickness of infiltrated tephra, relative to the deposit thickness outside, varied from around 1–15% for the few buildings where measurements were made.

5 Discussion

5.1 Building damage

Blong (2003); Hayes et al. (2019), and Williams et al. (2020) found a positive relationship between hazard intensity (tephra thickness, loading) and level of building damage at Rabaul 1994, Calbuco 2015, and Kelud 2014, respectively. This relationship is reflected in the development of building fragility functions used for impact forecasting (e.g., Pomonis et al., 1999; Spence et al., 2005; Jenkins et al., 2014; Maqsood et al., 2014). Spence et al. (1996) assessed buildings subjected to similar hazard intensity (~ 150 – 200 mm) during the 1991 Pinatubo eruption, Philippines, and found that the level of building damage varied with building

type (long-span *versus* short-span). Our findings in Ambae support both these previous findings, in that we identify a positive relationship between increasing tephra hazard intensity and increasing building damage states (Figure 7A) and, given similar tephra thicknesses, variation in the level of building damage as a function of building typology (Figure 8).

The performance of buildings at Ambae compared to previous damage surveys is difficult to compare because of i) building typology: the most comparable type, non-traditional timber-framed buildings (Nt), have high pitch metal sheet roofs in Ambae, compared to the low pitch of the similar building type (H) in Blong (2003) and the tiled and asbestos sheet roofs of Williams et al. (2020); and ii) the limited range of tephra thicknesses experienced by Nt buildings in Ambae; for example, metal sheet timber-framed roofs (built to snow loading code: Hayes et al., 2019) impacted by <100 mm from Calbuco represent 18% or 30% of the total Calbuco dataset ($n = 327$ or $n = 396$, depending on the tephra isopachs used) compared to 91% of the Ambae Nt dataset ($n = 43$; Figure 7D).

While no damage surveys have previously been carried out for the traditional short-span (Ts) buildings that are prevalent on Ambae, vulnerability estimates have been developed for comparable nipa thatch buildings in the Philippines. Discussions with residents of such buildings in Ambae and the Philippines noted that materials used in traditional buildings degraded in quality over time and it was expected that most buildings would be rebuilt every 7–10 years due to this, meaning that the building age and condition was considered

TABLE 3 Ambae building categories, codes used, and subcategories developed for the inventory of 589 buildings. The number of buildings in each main category, and the percentage of the total surveyed building stock, are shown in brackets in the first column.

| Category | Code | Construction subcategory | Number | Description |
|---|------|---|--------|---|
| Traditional [n = 259; 44%] | Ts | Traditional short span | 255 | Primarily wooden posts with bamboo for wall and roof framing, typically split bamboo wall cladding and high pitch thatched roof cover (may have additional corrugated sheet metal and/or may have no wall cladding) |
| | To | Traditional outhouse | 4 | Same as Ts but smaller (one occupant) with flat roof |
| Hybrid construction [n = 103; 17%] | X1 | Modern wall, traditional roof | 7 | Timber framed wall, typically corrugated sheet metal cladding and traditional roof as described in Ts |
| | X2 | Traditional wall, modern roof | 20 | Timber framed roof, typically with corrugated sheet metal cover with traditional wall frame as described in Ts |
| | Xw | Mixed construction | 76 | Unreinforced breeze block basal wall frame and remaining half timber, typically split bamboo cladding, or metal sheet, with a timber framed roof with corrugated sheet metal cladding |
| Non-traditional construction [n = 214; 36%] | Nt | Timber frame | 47 | Timber framed walls and roof, high pitch corrugated sheet metal roof and typically timber, plywood or corrugated sheet metal walls |
| | Nb | Unreinforced concrete block masonry | 161 | Unreinforced breeze block masonry walls, a timber framed roof and corrugated sheet metal roof cover |
| | Nc | Reinforced concrete frame | 6 | Reinforced concrete wall frame (with or without breeze block infill walls) with a timber framed roof and corrugated sheet metal roof cover |
| Temporary shelter [n = 13; 2%] | E | Temporary structure used for evacuation | 13 | Fibreglass frame with a canvas cover tied down with rope |

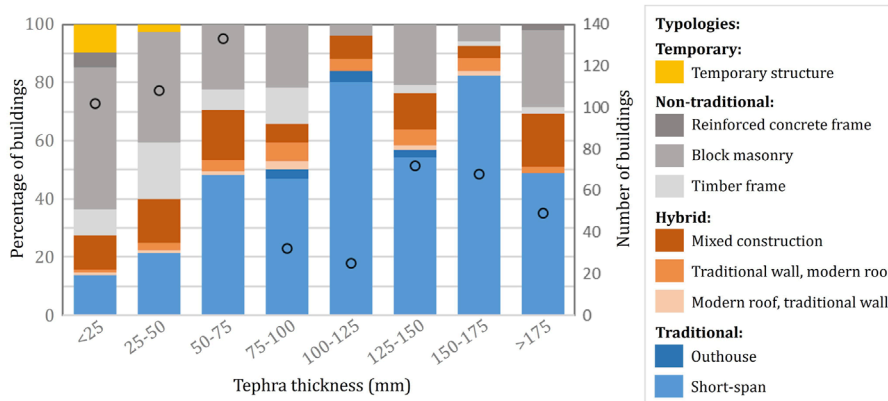


FIGURE 6 Building typology for all 589 assessed buildings, as a function of tephra thickness. Number of buildings are shown on the second y-axis as black hollow circles. Colour groupings - blue, orange, grey, yellow - indicate the main building type categories - traditional, hybrid, non-traditional, and temporary, respectively.

TABLE 4 The distribution of the number of buildings damaged based on their construction sub-category. Values in brackets are the integer percentage of buildings of that subcategory that are in that damage state, except for the brackets in the 'Total' row, which show the percentage of buildings in each damage state category.

| Construction classification | | | Damage state | | | | | |
|------------------------------|----|-----------------------------------|--------------|-----------|---------|---------|--------|----------|
| | | | DS0 | DS1 | DS2 | DS3 | DS4 | DS5 |
| Traditional | Ts | Short span | 94 (37%) | 73 (29%) | 19 (7%) | 10 (4%) | 4 (2%) | 55 (22%) |
| | To | Outhouse | 3 (75%) | 1 (25%) | 0 (0%) | 0 (0%) | 0 (0%) | 0 (0%) |
| Hybrid construction | X1 | Modern wall, traditional roof | 5 (71%) | 2 (29%) | 0 (0%) | 0 (0%) | 0 (0%) | 0 (0%) |
| | X2 | Traditional wall, modern roof | 9 (45%) | 1 (5%) | 2 (10%) | 2 (10%) | 0 (0%) | 6 (30%) |
| | Xw | Mixed wall construction | 48 (63%) | 13 (17%) | 8 (11%) | 3 (4%) | 1 (1%) | 3 (4%) |
| Non-traditional construction | Nt | Timber frame | 32 (68%) | 10 (21%) | 2 (4%) | 2 (4%) | 0 (0%) | 1 (2%) |
| | Nb | Unreinforced breeze block masonry | 126 (78%) | 31 (19%) | 2 (1%) | 1 (1%) | 1 (0%) | 0 (0%) |
| | Nc | Reinforced concrete frame | 5 (83%) | 1 (17%) | 0 (0%) | 0 (0%) | 0 (0%) | 0 (0%) |
| Temporary shelter | E | Temporary structure | 10 (77%) | 2 (15%) | 1 (8%) | 0 (0%) | 0 (0%) | 0 (0%) |
| Total | | | 332 (56%) | 134 (23%) | 34 (6%) | 18 (3%) | 6 (1%) | 65 (11%) |

key to its vulnerability. Jenkins et al. (2014) proposed nipa thatch fragility functions that forecast roof collapse (DS4/5) at between 1 and 2.1 kPa (10th to 90th percentile), with a mean of 1.4 kPa. Blong (1984) also proposed 100 mm as a thickness threshold for failure of weak buildings. Assuming an average tephra density of 1,000 kg/m³ based on the laboratory- and field-measured densities on Ambae, this corresponds to 80% of DS4/5 Ts buildings being impacted by tephra thicknesses between 100 and 210 mm. For Ambae, 65% (38 out of 59) of DS4/5 Ts buildings fall within those tephra thickness bounds, with 75% (44 out of 59) lying between 99 mm and 215 mm. The mean tephra thickness for Ts DS4/5 buildings on Ambae is 136 mm (c. 1.36 kPa), remarkably close to the 1.4 kPa proposed by Jenkins et al. (2014). This suggests that the expert-judgement derived fragility functions match well the observed damage on Ambae, giving some confidence in their application to impact forecasting in other areas. Ideally, vulnerability functions combine all data, i.e., empirical with theoretical, experimental, and expert judgement, as well as communicating the uncertainty in the estimate.

For hybrid and non-traditional buildings with corrugated sheet metal roofs (X2, X2, Nt, Nb, Nc), the level of damage sustained differed according to the condition and likely age of the roof and roof support. Figure 9A shows a hybrid building of non-traditional walls with traditional roof (X1); the building on the left has sustained collapse of the primary apex roof beam, while the building on the right remains intact. Both buildings were constructed at the same time and subjected to the same tephra thickness (~47 mm), with the only difference being that the collapsed building was constructed with a bamboo apex roof beam and the intact building with squared

timber. This shows the importance of evaluating all components of a building in impact assessment and forecasting. Where that is not feasible (for example, false ceilings or plastered walls covering components) it is important that the uncertainty associated with the vulnerability components of impact forecasts is quantified and communicated.

5.1.1 Building failure modes

Of those buildings that suffered collapse (DS5; n = 65, Table 4), most (n = 55) were traditional short-span buildings (Ts). There were three main modes of failure for this building type:

1. Failure of the vertical load-bearing props supporting the edge or apex line of the roof (Figure 9B);
2. Failure of the primary horizontal apex roof beam (purlin: Figure 9C);
3. Detachment or failure of the principal rafters (running downslope from the primary apex roof beam: Figure 9D).

These mechanisms (plus failure of the roof covering only, as we observe in non-traditional buildings on Ambae) have all been identified as previously observed failure mechanisms in a summary of significant recorded tephra fall impacts from 27 eruptions by Spence et al. (2005). While we did not have information on building age to enable analysis, residents in Ambae considered that only the older buildings were collapsing due to degraded quality of the structural elements.

Good condition sheet metal roofs showing no corrosion exhibited collapse of the roof and/or support structure (Figure 10A) with destabilisation of the walls. For poor condition and corroded

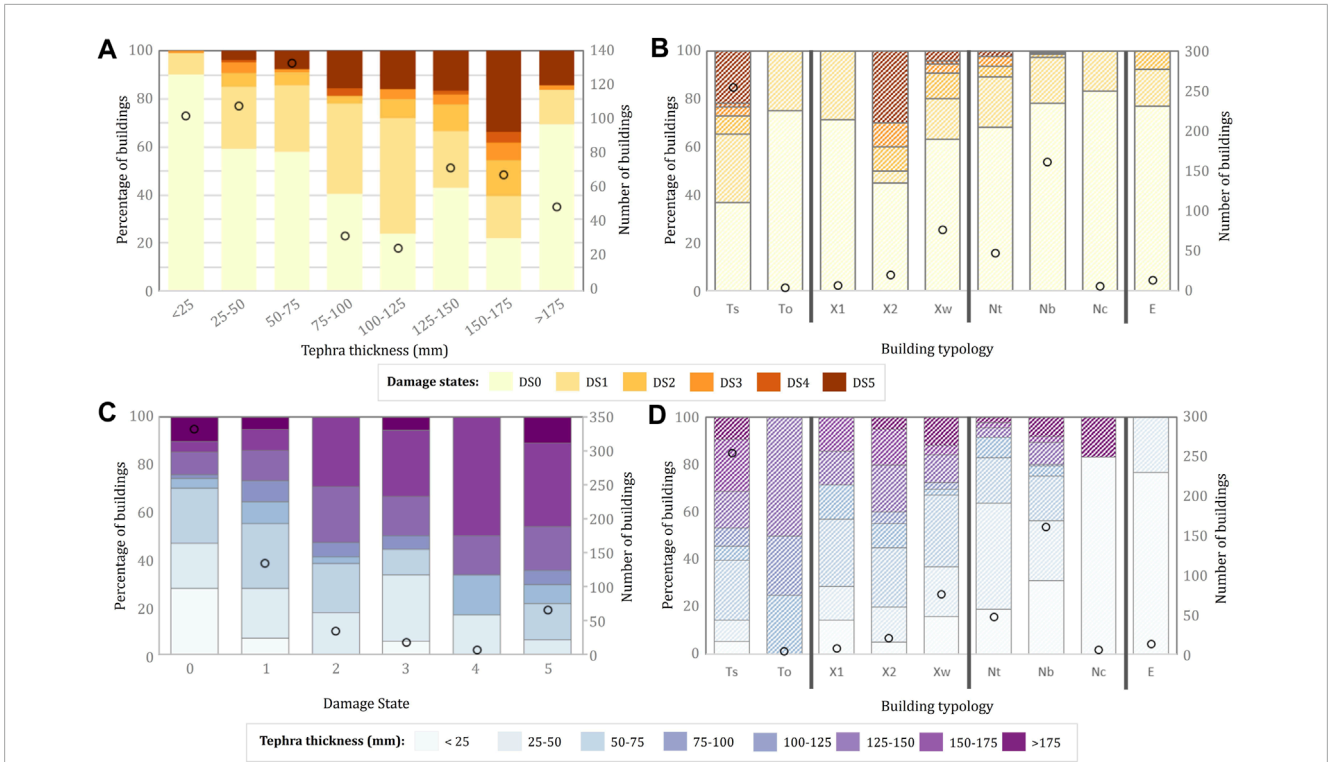


FIGURE 7 Damage states relative to tephra thickness and building typology (see Table 3 for code descriptions) for the 589 assessed buildings, shown as (A) the proportion of different damage states with increasing tephra thickness; (B) The proportion of damage states as a function of building typology; (C) Proportion of different tephra thickness bins with increasing damage state, and (D) proportion of different tephra thickness bins as a function of building typology. The bars in plots b and d are hashed to distinguish them from a and c, but follow the same legend. Hollow black circles show the number of data (second y-axis) and vertical black lines in b and d delineate the broad building typologies.

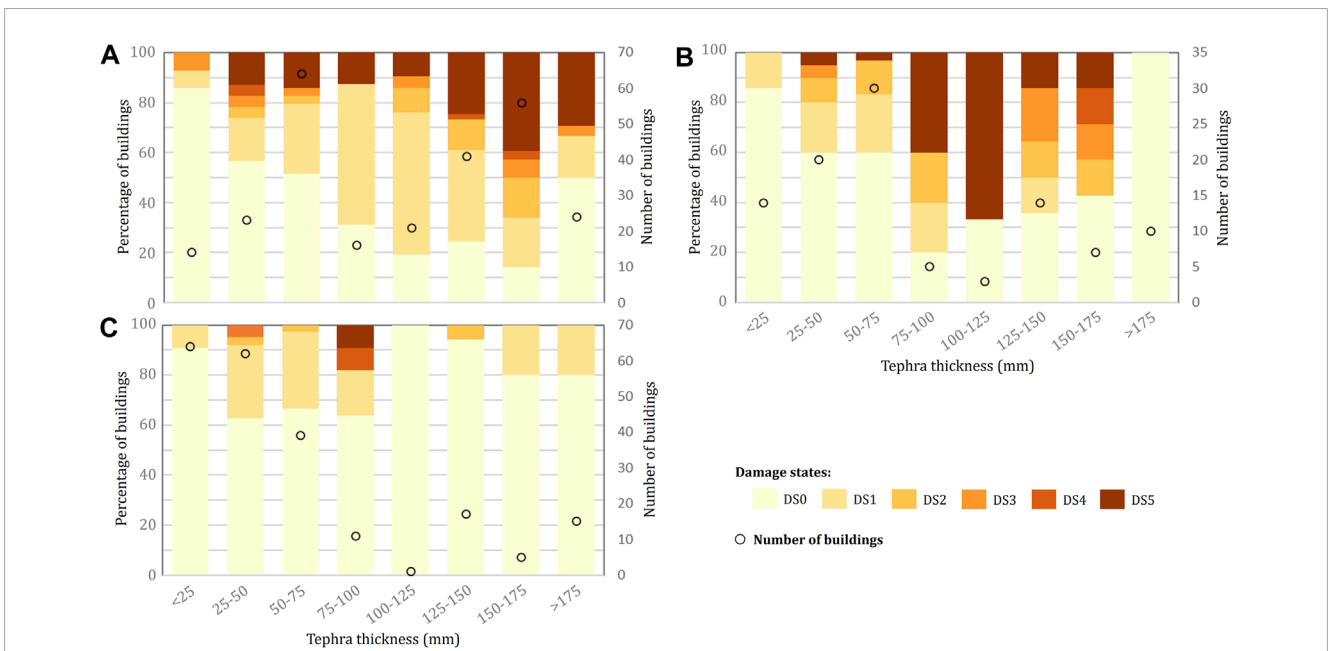


FIGURE 8 Proportion of damage states as a function of tephra thickness, for the three main typology categories: (A) Traditional (Ts, To); (B) Hybrid (X1, X2, Xw); (C) Non-traditional (Nt, Nb, Nc). Number of surveyed buildings in each bin are shown on the second y-axis as black hollow circles (note the axis limit for number of buildings in b) is half that of (A) and (C)). Temporary shelters (n = 13) are not shown.



FIGURE 9

(A) Two hybrid buildings subjected to ~47 mm tephra fall show full (left) and no (right) roof collapse as a result of different materials used for the primary apex roof beam; and complete collapse of traditional (Ts) buildings, where (B) the vertical load-bearing props (tree trunks) have snapped at their base (tephra thickness ~55 mm); (C) the primary apex roof beam has broken but the vertical load-bearing props remain intact (tephra thickness ~53 mm); (D) where the vertical load-bearing props and apex beam remain intact (in the front section of the building), but the principal rafters are detached and damaged (tephra thickness ~134 mm). All photos: S.F. Jenkins.

sheet metal roofs, failure was typically through the roof covering, with the roof support structure remaining intact (Figure 10B). This has implications for the repair costs of such buildings in areas where tephra thicknesses are large enough to cause failure of good condition metal sheet roofs: more vulnerable poor condition metal sheet coverings will fail, preventing further tephra loading on the roof structure, while a good condition metal sheet covering may transfer all load to the roof support, which is more costly to repair than the roof covering alone in the event of failure. Conversely, a good condition metal sheet roof, which can be more difficult and costly to source than local timber, may be reusable. We observed at least one example of termite damage in the vertical load-bearing timber props of a non-traditional building (Figure 10C), which potentially would have exacerbated damage had the roof covering not been in very poor condition (resulting in failure of the roof covering).

5.2 Non-structural impacts

Gutters are an important but vulnerable feature of buildings on Ambae as 88% of households use private or shared rainwater storage tanks, most of which are fed by gutters, for their primary source of drinking-water (VNSO, 2016). Therefore, any damage to gutters can affect the habitability of an area. This is even more important for isolated communities that may not have the resources to quickly repair or replace damaged gutters. Hampton et al. (2015) carried out laboratory experiments of tephra loading on new PVC guttering designed to New Zealand building code and found minimum tephra fall thicknesses of around 120 mm and 270 mm

were required to cause gutter deformation or gutter failure on steep pitch roofs. This is higher than the thicknesses associated with gutter damage on Ambae, where 90% of the damage occurred with final tephra fall thicknesses of 18–167 mm, and the minimum thickness associated with damage was 1 mm. This is not unexpected given the new quality, design and number of fastenings used with the PVC guttering experiments of Hampton et al. (2015), but it does act to reinforce the importance of supplementing experimental data with empirical data, field observations, roof and gutter design, and context.

The proportion of tephra that infiltrates a building related to how well sealed a building was and the mobility of the tephra surface (i.e., moisture content), and is thought to also relate to meteorological conditions such as wind speed and atmospheric moisture, as well as tephra characteristics such as grain size and density. The ingress of tephra into the school at Lovunimbanga, where the windows and doors were closed, was through the gap between the external wall and the roof. Non-traditional buildings on Ambae, like many non-air-conditioned buildings in tropical environments, use this gap as a passive form of cooling, promoting turbulent air flow up the exterior of the building and allowing convective air flow through the building. However, this form of cooling provides a pathway for tephra suspended in the turbulent airflow to enter buildings and contaminate building interiors. Traditional buildings allowed ready ingress of tephra through the large ventilation gaps, thatched roofs and split bamboo wall material. Given more time to carry out a field survey, we would recommend a systematic collection of infiltrated tephra thicknesses, grain size characteristics, and potential pathways for ingress at surveyed buildings, to be compared with the tephra deposit outside and the atmospheric conditions during



FIGURE 10

Non-traditional buildings exhibiting (A) complete collapse (DS5) of the vertical load-bearing props with a good condition metal sheet roof covering (tephra thickness: ~134 mm); (B) a heavily corroded sheet metal roof resulting in DS3 damage (tephra thickness ~30 mm); and (C) termite damage to the vertical load-bearing prop.

and since deposition. The methods, speed, and costs of clean-up externally and internally are also valuable areas for future data collection.

5.3 Mitigation strategies

We observed a range of mitigation methods used by Ambae residents to minimise tephra fall impact on buildings (Figure 11); we discuss these in more detail over the following subsections.

5.3.1 Tarpaulin roof covers

Tarpaulins were used to cover roofs on 47 of the 589 buildings surveyed, 91% ($n = 43$) of which were traditional thatched roofs. The smooth surface of the tarpaulin allows tephra to shed more readily, particularly in contrast to the rough surface of traditional thatched roofs (Figure 11A), which retained tephra to a greater extent than corrugated sheet metal roofs, even after being cleared. Tarpaulins installed over thatched roofs were also reported to reduce tephra ingress through the roof. The use of tarpaulins to assist with tephra shedding was most prevalent in South Ambae, which received the thickest tephra falls. More than a quarter ($n = 36$) of all buildings in the region ($n = 135$) employed tarpaulin as a mitigation strategy, while tarpaulins were used for less than 10% of buildings in other areas of Ambae, where tephra thicknesses were lower.

5.3.2 Removal of gutters

Of the 589 buildings surveyed on Ambae, 58 had gutters, with a further 35 showing evidence of having had gutters removed (Figure 11B) (93 total). The pre-emptive removal of guttering can prevent both damage to the gutter from overloading, as tephra is washed off the roof, and the contamination of water supplies. Rainwater tanks are the primary water source for Ambae residents, with many tanks fed by gutters.

5.3.3 Reinforcement of roof support structure

We observed floor “propping” poles that provided additional support to the primary beams (Figure 12) in two buildings in our survey. Conversations with one of the building owners confirmed that poles were placed to reinforce the primary beam and roof frame under tephra loading. Such poles increase the tephra loading that a roof can withstand: Figure 12 shows a hybrid building (Xw) that was exposed to ~125 mm of tephra during the July 2018 tephra falls. The building suffered extensive bending of the corrugated sheet metal roof cover and snapping of the supporting purlins/rafters, and yet the roof structure did not collapse, presumably because of the pole propping the roof from the floor in the centre of the building providing additional support. The potential benefit of temporarily propping or bracing roofs to increase their tephra load bearing capacity has been previously considered by Spence et al. (2005). These studies assumed that with carefully installed props the weakest building types could more than double their load bearing capacity, and accordingly, modelling the use of such props led to



FIGURE 11
Mitigation strategies employed by residents on Ambae to limit the impact of tephra falls on buildings: **(A)** successful use of a tarpaulin over part of a roof in south Ambae in shedding tephra; **(B)** Pre-emptive removal of guttering to prevent gutter damage and/or contamination of water supply; **(C)** Length of guttering used to clear tephra off roofs on Ambae; **(D)** Covering of large openings on traditional buildings in order to limit tephra contamination of the interior.

large reductions in building damage estimates. While this study provides only two examples of props being used, these suggest that a single prop may act to increase the load bearing capacity of an entire roof, but that moderate damage can still occur, especially in the roof covering, even if props have prevented roof collapse. The fact that propping was attempted by so few residents suggests that propping was either not widely considered as a mitigation option, or that the act of propping is not straight-forward to carry out; from discussions in the field this was driven by time-constraints prior to evacuation, rather than a lack of suitable available materials.

5.3.4 Roof cleaning

That tephra had been cleaned from roofs was visible in the contrast in deposit thickness and stratigraphy between the building roof and nearby floor. Techniques for cleaning varied depending on whether the roof cover was traditional thatched or corrugated sheet metal. It was reported that traditional thatched roofs were typically cleaned from the ground with long-handled brooms or with brooms and rakes from the roof by lighter people such as children. For corrugated sheet metal roofs, observed cleaning implements included plastic half-pipes, lengths of guttering (Figure 11C) and home-made rakes with inbuilt corrugations, in addition to the brooms used for thatched roofs.

5.3.5 Reducing contamination of interiors

Attempts to prevent or limit tephra contamination in buildings mostly involved covering building openings and windows with tarpaulins or cloth (Figure 11D). We did not observe any attempts

to block the ventilation gaps between external walls and roofs. In Lolopuepue village, 17 km northeast of the vent, coconut leaves were placed over unconsolidated tephra deposits in an area of high foot traffic to suppress remobilisation.

In future, with a larger number of data, by consistently taking note of the buildings that did or did not employ various mitigation strategies (not possible here because of time constraints), we would assess their effectiveness in limiting impacts from tephra, providing a stronger evidence base for future mitigation strategies.

5.4 Limitations

Post-eruption building damage surveys typically do not evaluate every building affected by tephra fall because of limits on time, access, and resources. They may focus on the more damaged buildings, the more strategic areas or buildings (e.g., for rehabilitation), or those closest to access routes. Thus, the surveyed damage distribution may not represent the total damage distribution from a tephra fall. For example, timber-framed metal sheet roofs (Nt) are predominantly not damaged (DS0: 68%), while traditional short span buildings (Ts) are predominantly damaged (DS1-5: 63%, Table 4); however, only 9% of Nt buildings experienced tephra thicknesses >100 mm compared to 55% for Ts (Figure 7D). This likely reflects different typologies being prevalent in different parts of the island but a full building survey could confirm this. Surveying buildings across a range of tephra thicknesses is not always possible because of constraints on data (Spence et al., 1996),



FIGURE 12

Hybrid building exposed to ~125 mm of tephra during the July 2018 eruption phase: (A) exterior of the building with visible bending in the corrugated metal sheet roof cover. (B) Snapped purlin/rafter and deformed roof covering. (C) Prop installed to reinforce the roof support structure along with extensive bending in the roof cover and purlins/rafters.

time, geography (i.e., for islands), or the distribution of buildings and building types relative to tephra falls (as at Ambae). As more surveys are undertaken, including through remote sensing, more data will supplement individual surveys to allow data to be aggregated across surveys, according to similar building types (e.g., as has been done for earthquakes: Spence et al., 2011).

Tephra fall thicknesses at the building scale were mostly interpolated from isopachs developed from in-field thickness measurements. Tephra measurements and surveyed buildings were only co-located in nine instances; however, isopach-interpolated thicknesses match well with those measured in the field. As there is some uncertainty around the tephra thickness assigned to each building we assess damage relative to binned ranges, rather than discrete values, of tephra thickness. We assume that buildings impacted by more than one tephra fall were cleaned (by humans or environmental actions) between tephra falls, in line with our observations during multiple field visits. However, it is possible that this was not the case for all buildings, and it is also possible that for the traditional roof materials some of the tephra may have infiltrated into the thatch and remained within the roof covering despite surface cleaning. This would have the effect of correlating damage (or lack of damage) with smaller thicknesses in our impact assessment, ultimately leading to conservative estimates of damage. Conversely, as highlighted by Blong (2003), the threshold at which a building sustains damage may be lower than that recorded in the field (as tephra may have continued to accumulate after damage had occurred). We also acknowledge that the time interval between deposition and measurement, as well as the climate and environment

and topographic setting of the deposit, may have resulted in different tephra fall thicknesses and densities than we report here. Specifically, thicknesses will decrease through erosion or compaction, and compaction will increase density (and thus load). Measured tephra thicknesses may have been affected by compaction and/or erosion, potentially leading to an underestimation of deposited load and thickness in the east where tephra 'crusts' were observed. Previous field-based experiments from Blong et al. (2017) demonstrated that within 1 week of deposition, rainfall can drive high levels of deposit compaction ($\geq 30\%$), although laboratory rainfall experiments by Tarasenko et al. (2019) and Williams et al. (2021) found heavy rainfalls caused negligible amounts of deposit compaction ($< 5\%$) with Williams et al. (2021) finding density increases of up to 30% under heavy sustained rainfall. The challenges associated with robustly and accurately characterising tephra fall deposits are well documented (Engwell et al., 2013), and our resulting analysis of how tephra fall deposits correlate with building impacts unavoidably incorporates some of these uncertainties, with tephra fall thickness estimates likely to be more conservative (i.e., underestimated) than less conservative (i.e., overestimated).

6 Conclusion

The 2017/2018 eruption of Manaro Voui volcano, Ambae, had two major tephra fall phases (March/April and July 2018) that damaged buildings. Critical impacts included building collapse, heavy damage to crops, contamination of water supplies, and

reworking of tephra deposits by dry season trade winds. During three field visits in April, July and August 2018, we recorded the location, building characteristics, and level of tephra fall damage for 589 buildings. We found a clear relationship between increasing tephra fall thickness and increasing damage severity and in the response of different building types to the same tephra thicknesses. The lowest thresholds of tephra fall generating collapse for traditional, hybrid, and non-traditional construction were 38 mm, 32 mm and 97 mm, respectively. Four modes of building collapse were observed: failure of vertical load-bearing posts at the edge or apex line of the roof, failure of the primary horizontal apex roof beam, detachment or failure of the principal rafters, and failure of the roof covering. Non-structural damage to guttering systems was commonly observed on non-traditional buildings. Pre-emptive removal of gutters was observed, preventing their overloading from tephra washed from the roof, and preventing tephra contamination of water supplies by ingress into rainwater storage tanks and wells.

Despite the relatively low tephra thicknesses generating collapse, some buildings sustained no damage in areas exposed to >200 mm, potentially related to mitigation strategies such as tarpaulin roof covers and/or reinforcement of the horizontal apex roof beam. Tarpaulin covers represent a relatively cheap and effective method for minimising building damage from tephra loading by assisting tephra shedding, particularly for the thatched roofs that can retain tephra. However, tarpaulins were rarely large enough to cover a whole building, and some had clearly been placed between phases or during tephra falls. The safe implementation of mitigation strategies will depend on the number of buildings and resources, as well as if there is sufficient time to safely undertake any of the actions.

This empirical tephra fall building damage field dataset represents only the fourth such study published since 1995, supplementing the limited empirical data available for the development of fragility curves. It also provides the first empirical damage dataset for traditional timber thatch buildings, providing an evidence base for impact forecasts in the South Pacific.

Data availability statement

The datasets presented in this study can be found in online repositories. The names of the repository/repositories and accession number(s) can be found in the article/[Supplementary Material](#).

Author contributions

SJ: Conceptualization, Data curation, Formal Analysis, Investigation, Methodology, Supervision, Visualization, Writing–original draft, Writing–review and editing. AM: Conceptualization, Data curation, Formal Analysis, Investigation, Methodology, Visualization, Writing–original draft, Writing–review and editing. TW: Conceptualization, Investigation, Methodology, Project administration, Supervision, Writing–review and editing. CS: Conceptualization, Investigation, Methodology, Project administration, Supervision, Writing–review and editing. GL: Conceptualization, Investigation, Methodology, Project administration, Writing–review and editing. SC: Conceptualization, Investigation, Project administration, Writing–review and editing,

Methodology. EG: Conceptualization, Investigation, Project administration, Writing–review and editing, Methodology.

Funding

The author(s) declare that financial support was received for the research, authorship, and/or publication of this article. SJ acknowledges the AXA Joint Research Initiative and the Ministry of Education, Singapore, under its MOE Academic Research Fund Tier 3 InVEST project (Award MOE-MOET32021-0002) for funding support. This work comprises Earth Observatory of Singapore contribution number 578. We acknowledge funding from New Zealand's Ministry of Foreign Affairs and Trade and Resilience to Natures Challenge (Volcano).

Acknowledgments

Many thanks to the editor, Nick Varley, and two reviewers, Maurizio Mulas and Kazutaka Mannen, for their valuable feedback. We are grateful to the Vanuatu Meteorology and Geohazards Department for the opportunity to collaborate and the logistical support throughout this study. We thank the many residents of Ambae for sharing their experiences during the 2017/2018 Manaro Voui eruptive period and for providing our field teams with hospitality, transportation and assistance during their time on Ambae. We also thank Geoff Kilgour, Mike Rowe, Sally Dellow, Mike Rosenberg, Genna Campbell for field and laboratory support, and George Williams for fruitful discussions. We appreciate that each data point in this study represents an impact on a resident of Ambae; all images and data provided in this study have been approved for publication by the local agency responsible for monitoring geohazards in Vanuatu: The Vanuatu Meteorology and Geohazards Division.

Conflict of interest

The authors declare that the research was conducted in the absence of any commercial or financial relationships that could be construed as a potential conflict of interest.

Publisher's note

All claims expressed in this article are solely those of the authors and do not necessarily represent those of their affiliated organizations, or those of the publisher, the editors and the reviewers. Any product that may be evaluated in this article, or claim that may be made by its manufacturer, is not guaranteed or endorsed by the publisher.

Supplementary material

The Supplementary Material for this article can be found online at: <https://www.frontiersin.org/articles/10.3389/feart.2024.1392098/full#supplementary-material>

References

- Blong, R. (2003). Building damage in Rabaul, Papua New Guinea, 1994. *Bull. Volcanol.* 65, 43–54. doi:10.1007/s00445-002-0238-x
- Blong, R. J. (1981). "Some effects of tephra falls on buildings," in *Tephra studies. Proceedings NATO advanced studies Institute*. Editors S. Self, and R. S. J. Sparks (China: Laugarvatn and Reykjavik), 405–420. June 18–29, 1980.
- Blong, R. J. (1984). *Volcanic hazards. A sourcebook on the effects of eruptions*. Australia, Sydney, New South Wales: Academic Press.
- Blong, R. J., Grasso, P., Jenkins, S. F., Magill, C. R., Wilson, T. M., McMullan, K., et al. (2017). Estimating building vulnerability to volcanic ash fall for insurance and other purposes. *J. Appl. Volcanol.* 6 (2), 2. doi:10.1186/s13617-017-0054-9
- Craig, H., Wilson, T., Stewart, C., Villarosa, G., Outes, V., Cronin, S., et al. (2016). Agricultural impact assessment and management after three widespread tephra falls in Patagonia, South America. *Nat. Hazards* 82, 1167–1229. doi:10.1007/s11069-016-2240-1
- Cronin, S. J., Gaylord, D. R., Charley, D., Alloway, B. V., Wallez, S., and Esau, J. W. (2004). Participatory methods of incorporating scientific with traditional knowledge for volcanic hazard management on Ambae Island, Vanuatu. *Bull. Volcanol.* 66, 652–668. doi:10.1007/s00445-004-0347-9
- Deligne, N. I., Fitzgerald, R. H., Blake, D. M., Davies, A. J., Hayes, J. L., Stewart, C., et al. (2017). Investigating the consequences of urban volcanism using a scenario approach I: development and application of a hypothetical eruption in the Auckland Volcanic Field, New Zealand. *J. Volcanol. Geotherm. Res.* 336, 192–208. doi:10.1016/j.jvolgeoes.2017.02.023
- Deligne, N. I., Jenkins, S. F., Meredith, E. S., Williams, G. T., Leonard, G. S., Stewart, C., et al. (2022). From anecdotes to quantification: advances in characterizing volcanic eruption impacts on the built environment. *Bull. Volcanol.* 84 (1), 7. doi:10.1007/s00445-021-01506-8
- Dominguez, L., Bonadonna, C., Forte, P., Jarvis, P. A., Cioni, R., Mingari, L., et al. (2020). Aeolian remobilisation of the 2011-Cordón Caulle Tephra-Fallout Deposit: example of an important process in the life cycle of Volcanic Ash. *Front. Earth Sci.* 7, 343. doi:10.3389/feart.2019.00343
- Engwell, S. L., Sparks, R. S. J., and Aspinall, W. P. (2013). Quantifying uncertainties in the measurement of tephra fall thickness. *J. Appl. Volcanol.* 2 (1), 5. doi:10.1186/2191-5040-2-5
- Global Volcanism Program (2018a). "Report on Ambae (Vanuatu)," *Bulletin of the global volcanism network*. Editors Crafford, A. E., and Venzke, E. (China: Smithsonian Institution), 43, 2. doi:10.5479/si.gvp.bgvn201802-257030
- Global Volcanism Program (2018b). "Report on Ambae (Vanuatu)," *Bulletin of the global volcanism network*. Editors Crafford, A. E., and Venzke, E. (China: Smithsonian Institution), 43, 7. doi:10.5479/si.GVP.BGVN201807-257030
- Hampton, S. J., Cole, J. W., Wilson, G., Wilson, T. M., and Broom, S. (2015). Volcanic ashfall accumulation and loading on gutters and pitched roofs from laboratory empirical experiments: implications for risk assessment. *J. Volcanol. Geotherm. Res.* 304, 237–252. doi:10.1016/j.jvolgeoes.2015.08.012
- Hayes, J. L., Calderón, R., Deligne, N. I., Jenkins, S. F., Leonard, G. S., McSparran, A. M., et al. (2019). Timber-framed building damage from tephra fall and lahar: 2015 Calbuco eruption Chile. *J. Volcanol. Geotherm. Res.* 374, 142–159. doi:10.1016/j.jvolgeoes.2019.02.017
- Jenkins, S. F., Spence, R. J. S., Fonseca, J. F. B. D., Solidum, R. U., and Wilson, T. M., 2014. Volcanic risk assessment: quantifying physical vulnerability in the built environment, 276: 105–120. doi:10.1016/j.jvolgeoes.2014.03.002
- Jenkins, S. F., Wilson, T. M., Magill, C. R., Miller, V., Stewart, C., Blong, R., et al. (2015). "Volcanic ash fall hazard and risk. Chapter 3," in *Global volcanic hazards and risk*. Editors S. C. Loughlin, R. S. J. Sparks, S. K. Brown, S. F. Jenkins, and C. Vye-Brown (Cambridge, UK: Cambridge University Press), 173. Open Access and last accessed 01/12/2023 from: cambridge.org/volcano.
- Lechner, H. N., and Rouleau, M. D. (2019). Should we stay or should we go? Factors affecting evacuation decisions at Pacaya volcano, Guatemala. *Int. J. Disaster Risk Reduct.* 40, 101160. doi:10.1016/j.ijdr.2019.101160
- Maqsood, T., Wehner, M., Ryu, H., Edwards, M., Dale, K., and Miller, V. (2014). *GARI5 vulnerability functions: reporting on the UNISDR/GA se asian regional workshop on structural vulnerability models for the gar global risk assessment, 11–14 november, 2013*. Canberra, Australia: Geoscience Australia. Record 2014/38. Geoscience Australia: Canberra.
- Marti, J., Spence, R., Calogero, E., Ordoñez, A., Felpeto, A., and Baxter, P. (2008). Estimating building exposure and impact to volcanic hazards in Icod de los Vinos, Tenerife (Canary Islands). *J. Volcanol. Geotherm. Res.* 178 (3), 553–561. doi:10.1016/j.jvolgeoes.2008.07.010
- Martinez-Villegas, M. M., Solidum, R. U., Saludadez, J. A., Pidloano, A. C., and Lamela, R. C. (2021). Moving for safety: a qualitative analysis of affected communities' evacuation response during the 2014 Mayon Volcano eruption. *J. Appl. Volcanol.* 10, 6. doi:10.1186/s13617-021-00109-4
- Miller, V., Jenkins, S. F., Tennant, E., Johnson, M., Magill, C. R., and Wilson, T. M. (2023). "Building damage from tephra fall during the 2020–21 eruption of La Soufriere volcano," in Conference presentation at IAVCEI General Assembly, New Zealand, February 3, 2023 (Rotorua).
- Pomonis, A., Spence, R., and Baxter, P. (1999). Risk assessment of residential buildings for an eruption of furnas volcano, são miguel, the azores. *J. Volcanol. Geotherm. Res.* 92, 107–131. doi:10.1016/s0377-0273(99)00071-2
- Robin, C., Monzier, M., Crawford, A. J., and Eggins, S. M. (1993). The geology, volcanology, petrology-geochemistry, and tectonic evolution of the New Hebrides island arc, Vanuatu. IAVCEI Canberra 1993 excursion guide. *Aust. Geol. Surv. Org.*, 86.
- Roulund, D., Cisternas, A., Denkmann, R., Dufumier, H., Regnier, M., and Lardy, M. (2001). The December 1994 seismic swarm near Aoba (AMBAAE) volcano, Vanuatu, and its relationship with the volcanic processes. *Tectonophysics* 338 (1), 23–44. doi:10.1016/s0040-1951(01)00074-9
- Roovins, J., Stewart, C., and Brown, N. (2020). "Learning from population displacement in the Pacific: case study of the 2017–2018 eruption of Ambae volcano, Vanuatu," in *Disaster research science report 2020/04* (New Zealand: Massey University). Available at: <https://www.preventionweb.net/publication/learning-population-displacement-pacific-case-study-2017-2018-eruption-ambae-volcano>.
- Shultz, J. M., Cohen, M. Z., Hermosilla, S., Espinel, Z., and McLean, A. (2016). Disaster risk reduction and sustainable development for small island developing states. *Disaster Health* 3 (1), 32–44. doi:10.1080/21665044.2016.1173443
- Siebert, L., Cottrell, E., Venzke, E., and Andrews, B. (2015). Earth's volcanoes and their eruptions: an overview. *Encycl. volcanoes*, 239–255. doi:10.1016/b978-0-12-385938-9.00012-2
- Spence, R., So, E., Jenkins, S., Coburn, A., and Ruffe, S. (2011). "A global earthquake building damage and casualty database," in *Human casualties in earthquakes*. Editors R. Spence, E. So, and C. Scawthorn (Germany: Springer), 339.
- Spence, R. J. S., Kelman, I., Baxter, P. J., Zuccaro, G., and Petrazzuoli, S. (2005). Residential building and occupant vulnerability to tephra fall. *Nat. Hazards Earth Syst. Sci.* 5, 477–494. doi:10.5194/nhess-5-477-2005
- Spence, R. J. S., Pomonis, A., Baxter, P. J., Coburn, A. W., White, M., Dayrit, M., and Field Epidemiology Program Team (1996). "Building damage caused by the mount Pinatubo eruption of June 15, 1991," in *Fire and mud: eruptions and lahars of mount Pinatubo, philip-pines. Philippine Institute of volcanology and seismology*. Editors C. G. Newhall, and R. S. Punongbayan (Seattle: University of Washington Press), 1055–1061.
- Tarasenko, I., Bielders, C. L., Guevara, A., and Delmelle, P. (2019). Surface crusting of volcanic ash deposits under simulated rainfall. *Bull. Volcanol.* 81 (30), 30. doi:10.1007/s00445-019-1289-6
- Vanuatu Meteorology and Geohazards Department (2018). Maewo response and recovery action plan, Ambae volcano. Available at: <https://reliefweb.int/report/vanuatu/vanuatu-maewo-response-recovery-action-plan-ambae-volcano>.

VNSO (2016). Vanuatu national statistics office 2016 post-tropical Cyclone pam mini-census report. Available at: <https://vnso.gov.vu/index.php/component/advertising/?view=download&fileId=4542>.

Warden, A. J. (1970). Evolution of aoba caldera volcano, new hebrides. *Bull. Volcanol.* 34, 107–140. doi:10.1007/bf02597781

Williams, G. T., Jenkins, S. F., Biass, S., Wibowo, H. E., and Harijoko, A. (2020). Remotely assessing tephra fall building damage and vulnerability: Kelud Volcano, Indonesia. *J. Appl. Volcanol.* 9 (1), 10–18. doi:10.1186/s13617-020-00100-5

Williams, G. T., Jenkins, S. F., Lee, D. W., and Wee, S. J. (2021). How rainfall influences tephra fall loading - an experimental approach. *Bull. Volcanol.* 83, 42–13. doi:10.1007/s00445-021-01465-0

Wilson, T. M., Cole, J. W., Stewart, C., Cronin, S. J., and Johnston, D. M. (2011). Ash storms: impacts of wind-remobilised volcanic ash on rural communities and agriculture following the 1991 Hudson eruption, southern Patagonia, Chile. *Bull. Volcanol.* 73, 223–239. doi:10.1007/s00445-010-0396-1

Zuccaro, G., Cacace, F., Spence, R. J. S., and Baxter, P. J. (2008). Impact of explosive eruption scenarios at Vesuvius. *J. Volcanol. Geotherm. Res.* 178 (3), 416–453. doi:10.1016/j.jvolgeores.2008.01.005